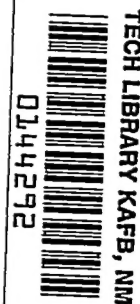


Copy 218  
RM L53I14a

NACA RM L53I14a



NACA

# RESEARCH MEMORANDUM

THE PERFORMANCE OF CONICAL SUPERSONIC SCOOP INLETS  
ON CIRCULAR FUSELAGES

By Lowell E. Hasel

Langley Aeronautical Laboratory  
Langley Field, Virginia

CLASSIFIED DOCUMENT

It is the policy of the National Advisory Committee for Aeronautics that no information contained herein shall be made available to an unauthorized person is prohibited by law.

NATIONAL ADVISORY COMMITTEE  
FOR AERONAUTICS

WASHINGTON  
November 17, 1953

NAAC 2876



## NATIONAL ADVISORY COMMITTEE FOR AERONAUTICS

## RESEARCH MEMORANDUM

## THE PERFORMANCE OF CONICAL SUPERSONIC SCOOP INLETS

## ON CIRCULAR FUSELAGES

By Lowell E. Hasel

The use of nose inlets in modern aircraft is restricted chiefly by the electronic equipment which must be located in the fuselage nose section or by the large amount of fuselage volume which the conventional nose-inlet installation requires. As a result, the inlet is usually located farther to the rear on the fuselage where it may be influenced by the fuselage flow field and boundary layer. Published research (refs. 1 and 2, e.g.) has shown that the fuselage boundary-layer air must not enter the inlet if the pressure recoveries of supersonic scoop inlets are to be comparable with the pressure recoveries of similar nose inlets. This research has, for the most part, been conducted on a flat plate at  $0^\circ$  angle of attack. At angles of attack, scoop-inlet characteristics may be expected to differ with position around and along the fuselage because of variations of the boundary-layer thickness and local flow field. Some angle-of-attack data are available (refs. 3 and 4, e.g.) but these data are not complete enough to enable a detailed evaluation to be made of scoop-inlet characteristics at angles of attack.

The Langley Aeronautical Laboratory and the Lewis Flight Propulsion Laboratory of the National Advisory Committee for Aeronautics are concurrently investigating the angle-of-attack characteristics of scoop inlets using the models shown in figures 1 and 2. (Some of the results obtained at the Langley Laboratory are presented in ref. 5 and the results obtained at the Lewis Laboratory are presented in ref. 6.) Throughout the remainder of the discussion these configurations will be designated as models A and B, respectively. The inlets on both models are of the conical type, having  $25^\circ$  half-angle cones, and are designed for a Mach number of approximately 2. The inlet on model A has a capture area of about 25 percent of the fuselage frontal area. Model B utilizes two completely independent inlet and diffuser systems. Each inlet is similar to the one illustrated in figure 2. The total capture area of the twin inlet installation is about 22 percent of the fuselage frontal area. On both models the splitter plate separating the inlet from the boundary-layer bleed is swept back from the tip of the central body to the lip of the inlet. The boundary layer is removed by means of a suction bleed on model A; whereas on model B a  $16^\circ$  included-angle wedge diverter is used to displace the boundary layer around the sides of the inlet. The tip of the wedge is located at the same axial position as the tip of the

file 2870

central body. Provisions are incorporated in both configurations for varying the bleed height. On model A the maximum bleed height is twice that illustrated in figure 1. The fuselage forebody fineness ratios of model A are 4.0 and 6.5. The nose section is an ogive of fineness ratio 3.5. The forebody of configuration B has a fineness ratio of 7.5 and corresponds to the RM-10 forebody shape.

Before discussing the test results, a brief review will be given of those features of the flow about bodies of revolution (ref. 7) at angles of attack which influence scoop performance.

At angles of attack the boundary layer flows from the windward to the leeward side of the fuselage, figure 3, thus reducing the thickness on the bottom and increasing the thickness on top. As the angle of attack increases the boundary layer separates and creates a stable vortex pattern similar to that known to exist under certain conditions behind circular cylinders. The angle of attack at which the vortices are first evident at the inlet varies with axial position of the inlet on the fuselage and the Reynolds number. A typical effect of the vortex formation is to thin the boundary layer over a small portion of the top of the fuselage. It is probable that on fuselages which are bodies of revolution a portion of these vortices will enter an inlet located on the top section of the fuselage. If the angle of attack becomes very large, the vortex flow will become unstable. The latter condition may be expected to produce very unsatisfactory engine operation.

The forebody also has a significant effect, especially at angles of attack, on the local Mach number distribution at the inlet. High local Mach numbers and large cross-flow angles are created near the side of the fuselage; while on the bottom the local Mach number decreases.

The boundary-layer conditions which existed a short distance ahead of the inlets of models A and B at  $M = 2.0$  are illustrated in figure 4. The boundary-layer thickness expressed in terms of the boundary-layer thickness at  $0^\circ$  angle of attack is presented as a function of fuselage position. These data were obtained without the inlet installed on the fuselage. Transition wires were used on the two shorter forebodies to insure a turbulent boundary layer at the inlet, since this is the condition most likely to occur in flight. On the long forebody natural transition occurred upstream of the inlet. On the top section of the fuselages the increase of boundary-layer thickness at both angles of attack is smallest on the short forebody. (For reasons of clarity the boundary-layer data obtained on the long forebody at  $10^\circ$  have been omitted from fig. 4. The boundary-layer growth on this forebody at an angle of attack of  $10^\circ$  was greater than on the short forebody at  $12^\circ$ .) At  $6^\circ$  the vortex formation is evident only on the long forebody. At  $12^\circ$  a vortex has formed on the medium-length forebody but none is evident on the short forebody. On the bottom of the fuselages the boundary-layer thickness decreases considerably at angles of attack. It is interesting to note

that the vortex thins the boundary layer over only a relatively small portion of the top of the fuselage, and that this region of thin boundary layer appears to be too narrow to be utilized by typical inlets such as the one on configuration A.

Figure 5 presents a typical set of data obtained at  $M = 2.0$  from the configuration having the short forebody, showing the effect on pressure recovery of circumferential location of the inlet. Maximum pressure recoveries are presented as a function of fuselage position and angle of attack. The bleed-height ratio,  $h/\delta_{\alpha=0}$  of 1.25, chosen for this figure represents the ratio of the boundary-layer bleed height to the boundary-layer thickness at  $0^\circ$  angle of attack. Preliminary examination of the data has indicated that the bleed system was removing all of the air which could enter its capture area. The maximum pressure recovery is adversely affected by angle of attack if the inlet is located anywhere in the region extending from the top to the side of the fuselage. These losses are caused either by the thickening of the boundary layer, high local Mach number and accompanying large cross-flow angles, or a combination of the two effects. On the bottom of the fuselage the pressure recovery increases with angle of attack because of the decrease in local Mach number ahead of the inlet.

The effect of bleed height on scoop performance is illustrated in figure 6 which presents the maximum pressure recoveries as a function of bleed-height ratio for three angles of attack and for three inlet positions. At  $0^\circ$  the pressure recovery continues to increase when the bleed-height ratio exceeds 1. This is possibly due to the fact that, as the bleed height increases, the average Mach number of the air entering the inlet decreases slightly. When the inlet is on top of the fuselage, the pressure recovery at  $6^\circ$  continues to increase until the bleed-height ratio is about equal to the maximum boundary-layer thickness ratio. At  $12^\circ$  the pressure recovery appears to become constant at a bleed-height ratio near 2 although the maximum boundary-layer thickness ratio is about 3.7. At the side position, increasing the bleed-height ratio has less beneficial effect on the pressure recoveries at angles of attack since the losses are primarily caused by high local Mach numbers and large cross-flow angles. At the bottom position the bleed height has only a small effect on the pressure recovery of the inlet.

These pressure-recovery characteristics (figs. 5 and 6) at angles of attack may be expected to change to some extent with forebody length. The variations will be greatest at the top inlet position because of the differences in the rate of boundary-layer thickening (fig. 4) and because of the vortex formation which may exist at an inlet mounted farther to the rear on a fuselage.

The effect of forebody length on pressure recovery is illustrated in figure 7. The pressure recoveries, expressed in terms of the  $0^\circ$  recovery, are presented as a function of angle of attack for the top and bottom inlet positions. The bleed-height ratio is 1.25. The effect

of the more rapid thickening of the boundary layer on the top of the two longer forebodies is most evident at moderate angles where the decrease in pressure recovery of these configurations is appreciably more than for the short body configuration. At the higher angles of attack an abrupt and favorable change in the scoop characteristics on the longer forebody occurs, probably because of the effect of the vortices generated on this forebody. On the bottom of the fuselages, the effect of the forebody length is smaller. The reasons for the consistent variation of pressure recovery with forebody length have been investigated to some extent but no conclusions have as yet been reached. At larger bleed-height ratios the differences in the pressure recoveries for the top inlet configuration will probably decrease because a larger portion of the boundary layer on the longer forebodies will be removed.

If the forebody is long enough to produce a vortex flow ahead of the inlet, the variation of the pressure-recovery characteristics with bleed-height ratio will be somewhat different from those previously discussed. These differences may be noted in figure 8 which presents the recovery characteristics of an inlet mounted on top of the long forebody. On the left side of the figure the pressure recovery is presented as a function of the bleed-height ratio for several angles of attack. On the right side the distribution of the ratio of pitot pressure to free-stream total pressure on the fuselage just ahead of the inlet is shown for  $0^\circ$  and  $10^\circ$ . The free-stream value of this ratio is 0.72 at  $M = 2.0$ . The boundary-layer surveys indicated that the vortex formed on this forebody at the inlet station at about  $4^\circ$ . The action of the vortices is most evident when none of the boundary layer is removed from the inlet. At this condition the pressure recovery decreases as the angle of attack increases to  $3^\circ$ . Further increases of the angle of attack to  $6^\circ$  and  $10^\circ$  result in large increases in the pressure recovery. The pitot-pressure contours indicate that at  $10^\circ$  a relatively large amount of the vortex enters the inlet. It is thought that the primary effect of the vortex is to prevent separation of the boundary layer inside the inlet and thus increase the pressure recovery. As the bleed height increases, the pressure recoveries at the lower angles increase and the effect of the vortex becomes much less apparent.

Model B, which is the long forebody configuration (fig. 2), has also been tested at Mach numbers of 1.5 and 1.8. In general, the Mach number had little effect on the over-all pressure-recovery characteristics of the inlets. As the Mach number decreased the changes in pressure recovery with angle of attack also decreased.

It is obvious that the pressure-recovery characteristics of inlets operating on top of a fuselage can be improved if the boundary-layer thickness can be decreased. Several possible solutions to this problem exist in addition to methods such as minimizing fuselage angle of attack and keeping the inlet as far forward as is consistent with low-drag

considerations. The use of fuselages having noncircular cross-sectional shapes should be investigated. On fuselages of circular cross section, methods of producing a larger region of thin boundary layer should also be studied. If the transverse distance between the vortices can be increased and the vortices induced to form at smaller angles of attack, some benefit may result. This latter scheme has been briefly tried on configuration A by the use of axial and diagonal vortex-generator strips. To date, the desired increase in pressure recovery has not been obtained.

Figure 9 illustrates the drag characteristics of the top and bottom inlet positions. The external drag at a mass-flow ratio of about 0.9 is presented on the left side of the figure as a function of bleed-height ratio for angles of attack of  $0^\circ$  and  $6^\circ$ . At  $6^\circ$  the drag of the bottom inlet is higher than the drag of the top inlet. Since this difference in drag tends to counteract the pressure-recovery advantage of the bottom position the optimum location of the inlet should be determined on the basis of net thrust so that the effect of drag, as well as pressure recovery, may be considered. The maximum values of net thrust for a typical turbojet engine, expressed in terms of the net thrust at  $0^\circ$  are presented on the right side of the figure as a function of bleed-height ratio. In calculating the net thrust the assumption was made that the drag associated with the removal of the boundary-layer air was equal to one-half its kinetic energy. This assumption concerning the drag of the boundary-layer removal system is not critical to the net-thrust comparison because the bleed mass-flow ratios were about the same for the two inlet positions. It appears on the basis of net-thrust ratio that the top and bottom inlet positions are comparable for this particular configuration and angle of attack. It should be mentioned that this figure is based on preliminary data and may be subject to some changes after analysis of the data is complete. Nevertheless, it is important to note the compensating effects of drag and pressure-recovery characteristics which may exist for the top and bottom inlet positions.

Half-conical scoop inlets which are mounted on flat plates (refs. 2 and 8, e.g.) and have efficient boundary-layer-removal systems are essentially operating at free-stream conditions when the bleed-height ratio exceeds 1.0. Therefore, a comparison of the recoveries of these inlets and of practical scoop installations on a fuselage, such as A and B represent, is of interest to evaluate the recovery penalties which are associated with the fuselage installations. Such a comparison is made in figure 10 which presents, for an angle of attack of  $0^\circ$ , the maximum pressure recoveries of the flat-plate and fuselage-mounted inlets as a function of the bleed-height ratio. Since the flat-plate data were obtained at  $M = 1.88$  an estimate of the recovery of this inlet at  $M = 2.0$  has been made. The best recovery obtained from the fuselage configurations is about 4 percent less than the recovery of the flat-plate inlet. Between one-fourth and one-half of this loss is due to the fuselage nose shock



and the fact that the local inlet Mach number is higher than the free-stream Mach number. The cause of the remainder of the loss is not fully understood at present. There are some indications that the nonuniform velocity distribution at the inlet may be causing some of the additional loss. The difference which exists between the recoveries of the two shorter body configurations is considered to be due to slightly different local Mach numbers existing ahead of the inlet.

It is interesting to note (fig. 10) that the two entirely different systems of boundary-layer removal which were used on models A and B (figs. 1 and 2) gave essentially the same inlet pressure-recovery characteristics at a given bleed-height ratio. For a full-scale application, therefore, a diverter system similar to that used on model B appears to be more practical because of its aerodynamic simplicity, although some structural complications related to the support of the inlet floor may be involved. Characteristics of other satisfactory diverter systems may be found in references 2 and 8.

In conclusion, it appears that on circular fuselages the best pressure recoveries at angles of attack are obtained when a scoop inlet is located on the bottom of the fuselage. If the inlet must be placed on top, it should, in general, be located as far forward as is consistent with low-drag considerations. Location of a top inlet farther to the rear on a fuselage where it may be affected by the vortex flow will have a beneficial effect on the pressure recovery only if the boundary-layer bleed-height ratio is small and the angle of attack is large. The net thrust characteristics of top and bottom inlet installations may be comparable because of the compensating effects of the drag and pressure-recovery characteristics.

Langley Aeronautical Laboratory,  
National Advisory Committee for Aeronautics,  
Langley Field, Va., September 4, 1953.

## REFERENCES

1. Wittliff, Charles E., and Byrne, Robert W.: Preliminary Investigation of a Supersonic Scoop Inlet Derived From a Conical-Spike Nose Inlet. NACA RM L51G11, 1951.
2. Goelzer, H. Fred, and Cortright, Edgar M., Jr.: Investigation at Mach Number 1.88 of Half of a Conical-Spike Diffuser Mounted As a Side Inlet With Boundary-Layer Control. NACA RM E51G06, 1951.
3. Simon, Paul C.: Performance Characteristics at Mach Numbers to 2.0 of Various Types of Side Inlets Mounted on Fuselage of Proposed Supersonic Airplane. IV - Rectangular-Cowl Inlets With Two-Dimensional Compression Ramps. NACA RM E52H29, 1952.
4. Schaefer, Raymond F.: Some Design Configurations for Half-Round Side Inlets. Wright Aero Rep. No. 1692, Supersonic Inlet Symposium, Curtiss-Wright Corp. (Wood-Ridge, N. J.) Jan. 23, 1953.
5. Hasel, Lowell E., Lankford, John L., and Robins, A. W.: Investigation of a Half-Conical Scoop Inlet Mounted at Five Alternate Circumferential Locations Around a Circular Fuselage - Pressure-Recovery Results at a Mach Number of 2.01. NACA RM L53D30b, 1953.
6. Valerino, Alfred S., Pennington, Donald B., and Vargo, Donald J.: Effect of Circumferential Location on the Angle of Attack Performance of Twin Half-Conical Scoop-Type Inlets Mounted Symmetrically on the RM-10 Body of Revolution. NACA RM E53G09, 1953.
7. Allen, H. Julian, and Perkins, Edward W.: Characteristics of Flow Over Inclined Bodies of Revolution. NACA RM A50L07, 1951.
8. Piercy, Thomas G., and Johnson, Harry W.: A Comparison of Several Systems of Boundary-Layer Removal Ahead of a Typical Conical External-Compression Side Inlet at Mach Numbers 1.88 and 2.93. NACA RM E53F16, 1953.



LANGLEY SCOOP-INLET CONFIGURATION  
MODEL A

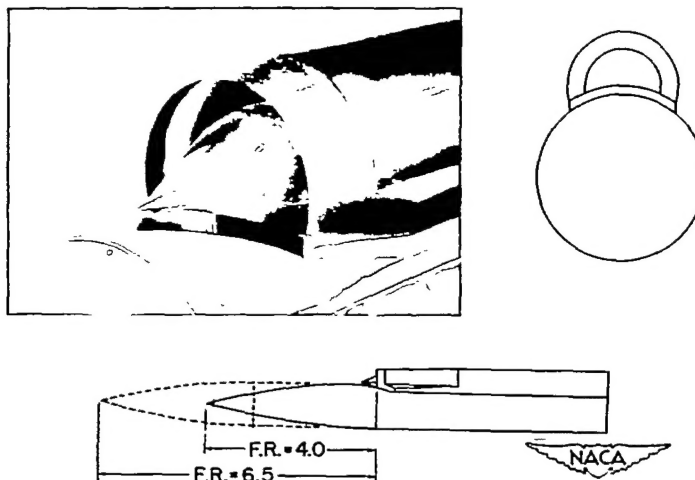


Figure 1

LEWIS SCOOP-INLET CONFIGURATION  
MODEL B

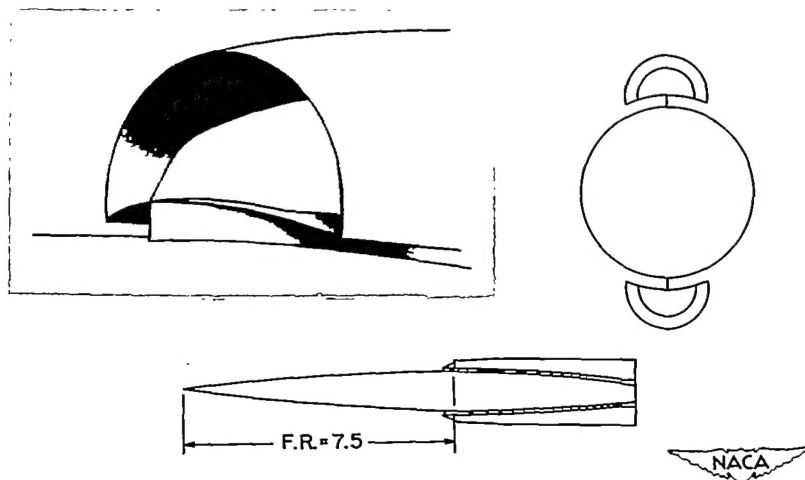


Figure 2

2Z

NACA RM L53I14a

9

# BOUNDARY-LAYER DISTRIBUTION ON A CYLINDRICAL FUSELAGE AT ANGLE OF ATTACK

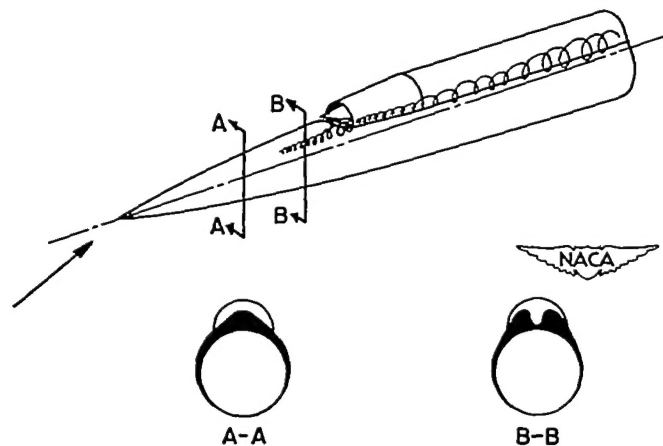


Figure 3

## EFFECT OF FOREBODY LENGTH ON BOUNDARY-LAYER THICKNESS AT ANGLES OF ATTACK M = 2.0

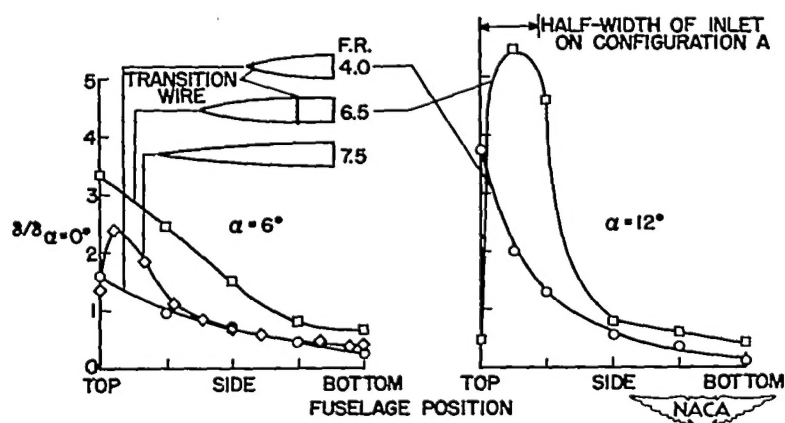


Figure 4

EFFECT OF INLET POSITION ON PRESSURE RECOVERY  
AT  $h/\delta_{\alpha=0^\circ} = 1.25$   
 $M = 2.0$

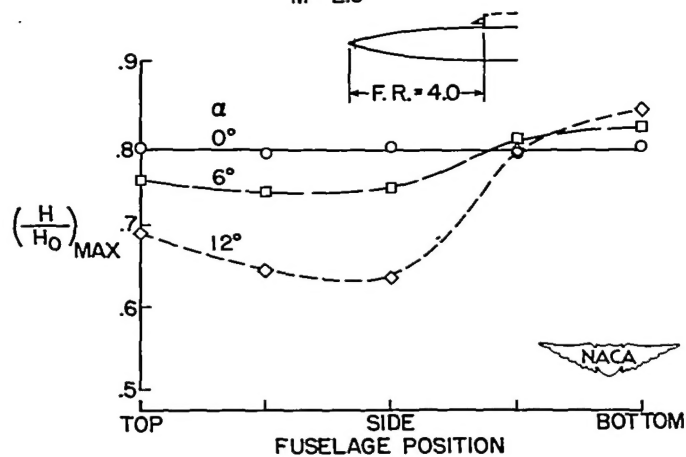


Figure 5

EFFECT OF BLEED HEIGHT ON PRESSURE RECOVERY

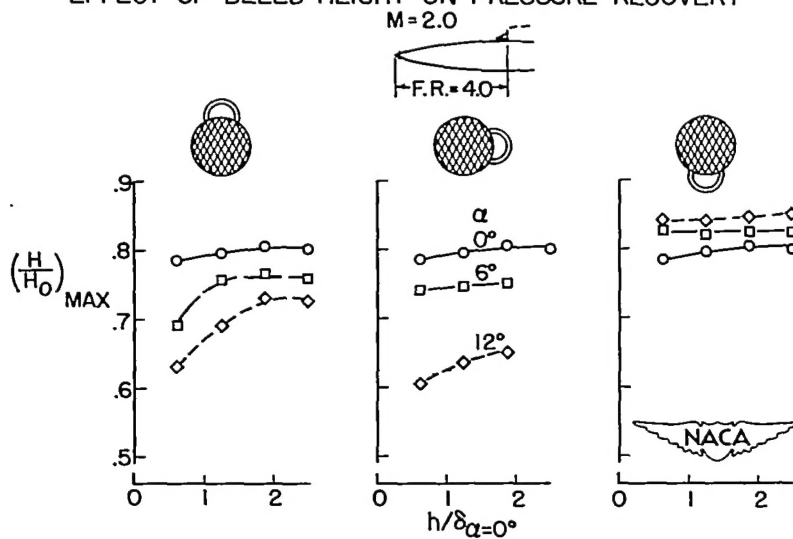


Figure 6

EFFECT OF FOREBODY LENGTH ON PRESSURE RECOVERY  
AT ANGLES OF ATTACK  
 $M=2.0$ ;  $h/\delta_{\alpha=0^\circ}=1.25$

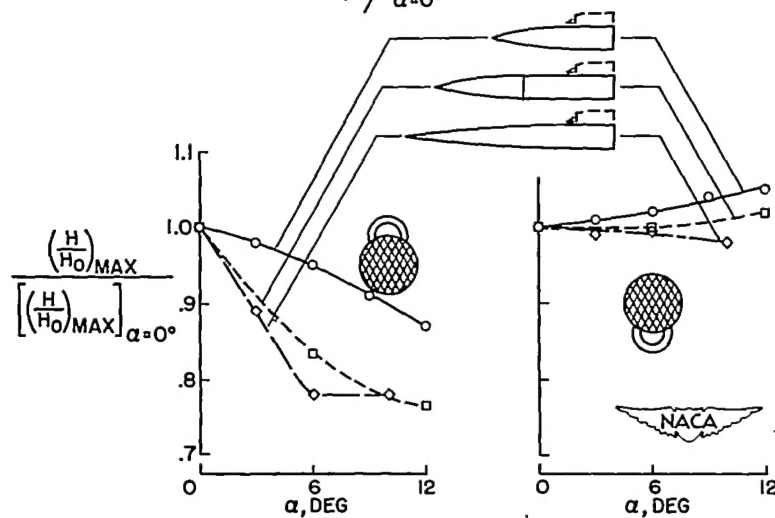


Figure 7

EFFECT OF FUSELAGE VORTEX ON PRESSURE RECOVERY  
 $M=2.0$

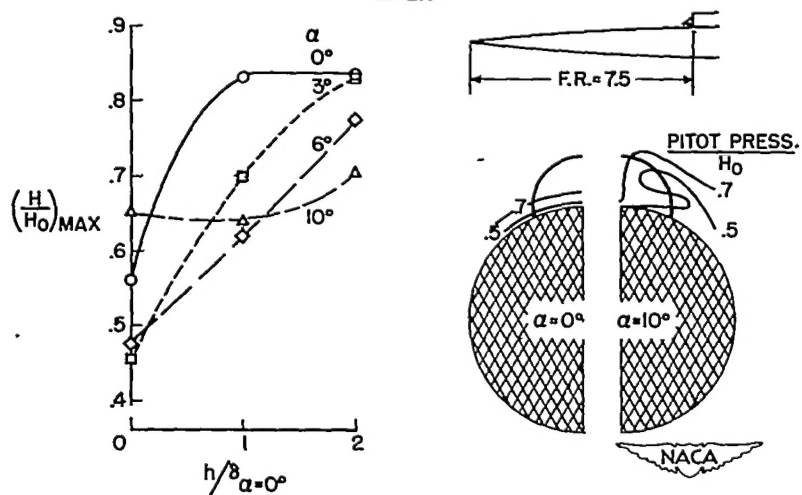


Figure 8

# EFFECT OF INLET POSITION ON NET THRUST

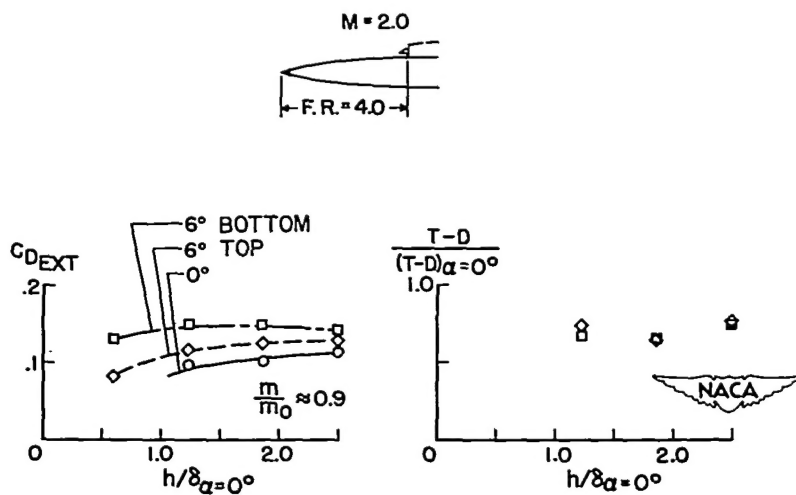


Figure 9

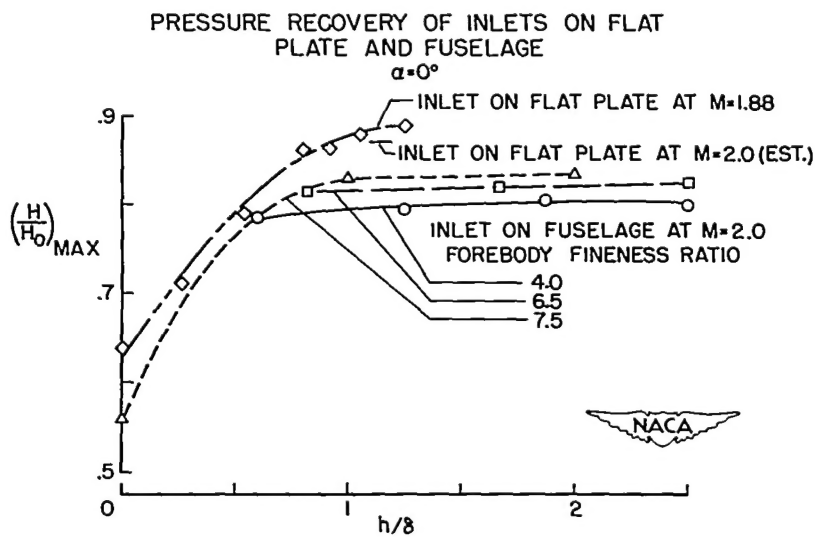


Figure 10